



ELECTRON SPIN RESONANCE DATING OF THE QUATERNARY FLUVIAL TERRACE SYSTEM OF THE UPPER HAN RIVER, CENTRAL CHINA

WENQIN DONG^{1,2,3,*}, SONG YU^{1,2,3}, QING HU^{1,2,3}, JIANCHAO WU^{1,2,3}, DONGNING LEI^{1,2,3}, YONGJIAN CAI^{1,2,3}

¹Institute of Seismology, CEA, Wuhan, Hubei 430071, China

²Hubei Key Laboratory of Earthquake Early Warning, Wuhan, Hubei 430071, China

³Hubei Earthquake Administration, Wuhan, Hubei 430071, China

Received: 28 August 2023

Accepted: 02 January 2024

Abstract

The geomorphology of the upper Han River, which is located in the southern Qinling Mountains (central China) and within the northern subtropical monsoon climate zone, contains abundant information on tectonic and climatic changes. Many Paleolithic sites are preserved in the Quaternary terraces in this region, making it an ideal area for studying both geomorphology and ancient human activity. However, owing to limitations in dating methods, the formation ages of the higher terraces T3–T5 of the upper Han River remain unclear. We collected 11 samples of sediment from the higher Quaternary terraces of Wufeng, Qingqu and the Yunyang Basin for electron spin resonance (ESR) dating of quartz grains. Results show that the formation ages of terraces T3, T4 and T5 are 422–401 ka, 627–621 ka and 1129–1099 ka, respectively. Integrating this information with the timings of documented climatic transitions and the history of regional uplift, we propose that the upper Han River terraces formed in response to the combined effects of climatic transition and tectonic uplift.

Keywords

terrace, upper Han River, ESR dating, early quaternary, tectonic landform, climate change

1. Introduction

River terraces are ancient river beds that have been preserved on the valley slope (Zhu *et al.*, 2022). The formation and geometry of terraces are known to be influenced by tectonic activity, climate change and erosion base level (Starkel, 2003). However, the process of terrace formation in inland areas is controlled mainly by tectonic uplift and climate change, as the influence of base-level variation on a river system is limited to the part of the river close to the estuary (Zeuner, 1935; Wang *et al.*, 2021). In areas influenced by strong tectonic uplift, such as the Qinling Mountains

of central China, river terraces are formed as a result of the combined action of tectonic uplift and climate change (Starkel, 2003; Tao *et al.*, 2018; Luo *et al.*, 2019). Both of the amplitudes of tectonic uplift and climate change deeply control the depth of river undercutting, whereas climatic characteristics mainly control the sedimentary process of terrace formation. River terraces in the Qinling Mountains are important geomorphological records of climatic and environmental change (Xue *et al.*, 2004; Pang *et al.*, 2014).

The Qinling Mountains, which extend across central China, represent a physical boundary between northern and southern China (Xue *et al.*, 2004). During the

Corresponding author: W. Dong
e-mail: dongwenqin1988@163.com.

late Cenozoic, the Qinling Mountains have been rapidly uplifted and eroded into an impressive landscape (Meng, 2017; Zhang *et al.*, 2019), and their formation has played a crucial role in shaping the physiography, climate, biological features and human activity of central China (Meng, 2017; Zhang, 2019). The Qinling Mountains are a transition zone between the temperate and subtropical climate zones and are highly sensitive to climate change. The Han River, which originates from Panzhong Mountain on the southern flank of the Qinling Mountains, is the largest tributary of the Yangtze River. Multiple river terraces are developed on both sides of the upper and middle sections of the Han River. These stepped river terraces preserve ancient fluvial sediments and form an important geomorphological record of the staged uplift of the Qinling Mountains and climatic change (Pang *et al.*, 2015; Mao *et al.*, 2017).

Previous geochronological research on the Han River has focused mainly on the lower-most and second-lowest terraces (T1 and T2; Huang *et al.*, 1995; Huang *et al.*, 1996; Chen *et al.*, 1997; Sun *et al.*, 2012, 2014; Pang *et al.*, 2013, 2017; Bahain *et al.*, 2017; Mao *et al.*, 2017; Zhu *et al.*, 2022). However, owing to limitations in dating methods and suitable geological materials, a systematic chronological framework and stratigraphic sequence for terraces higher than T1 and T2 have not been established, resulting in uncertainty regarding the chronostratigraphy of the terrace sequence. The lack of dating results has hindered the understanding of regional tectonic activity, climate change and long-term environmental change in the upper Han River area.

The electron spin resonance (ESR) dating method has been successfully applied to dating Quaternary fluvial and lacustrine sediments (Beerten *et al.*, 2006; Rink *et al.*, 2007; Voinchet *et al.*, 2007; Tissoux *et al.*, 2008, 2010; Voinchet *et al.*, 2010; Wei *et al.*, 2020, 2023). After detailed field investigations, three representative higher terrace profiles were selected from Wufeng County, Qingqu County and the Yunyang Basin in the upper section of the Han River for ESR dating to determine the chronology of terrace stepping and infer the controls on their formation.

2. Study Area and Sampling

The upper sections of the Han River are located in the southern Qinling Mountains in the northern subtropical monsoon climate zone and receive a mean annual precipitation of 870 mm (Pang *et al.*, 2015). This section of the Han River is ~925 km long and has a catchment area of 9.5×10^4 km². Gorges and basins are distributed alternately in this area. There are five levels of river terraces, T1–T5, in basins in the upper section of the Han River,

which are at +10+15 m (T1), +30+40 m (T2), +60+70 m (T3), +90+110 m (T4) and >+130 m (T5) above the current river bed, respectively (Zhu *et al.*, 1955). The lower terraces (T1 and T2) are widely distributed and well preserved, whereas the higher (T3–T5) terraces are cut, damaged and eroded to various extents and do not contain completely preserved accumulated fluvial–lacustrine sediments. This study focuses on terrace systems in Wufeng County (32°50′51.77″N, 110°22′16.97″E), Qingqu County (32°49′55.64″N, 110°34′43.63″E) and the Yunyang Basin (32°49′57.31″N, 110°44′53.98″E) in the upper section of the Han River (**Fig. 1**). The Wufeng and Qingqu terrace profiles are located on the left bank of the Han River, whereas the Yunyang Basin terrace profile is located on the right bank. Five terrace levels can be identified in each of these profiles (**Fig. 1**).

Of the five terrace levels, terraces T1 and T2 are accumulation terraces, whereas terraces T3–T5 are bedrock terraces partly covered by fluvial–lacustrine sediment. Detailed information about the three sampled terrace profiles is presented in **Fig. 2** and **Table 1**.

In this study, a total of 11 samples were collected. One sample was collected from each of T3, T4 and T5 in the Wufeng and Qingqu terrace profiles, and one sample from T4 and two from each of T3 and T5 in the Yunyang Basin terrace profile. The two samples from terraces T3 and T5 of the Yunyang Basin were collected to check the reliability and repeatability of our dating results.

3. Methods

3.1. Quartz Extraction

The quartz purification experiment was conducted at the Institute of Geology, China Earthquake Administration in Beijing, China, following the procedures described by Liu *et al.* (2010) and Wei *et al.* (2020). All the samples were separated into the 75–145 µm size fractions using wet sieving. The 75–145 µm size fraction has been identified as the most susceptible to optical bleaching during transportation (Voinchet *et al.*, 2015). Each sample was treated with 30% H₂O₂ for 24 h and with 40% HCl for 24 h to remove organic material and carbonates, respectively. After washing and cleaning with distilled water, the samples were subjected to heavy liquid separation (2.7 g/cm³) to remove heavy minerals, and mechanical magnetic selection to remove magnetic minerals. In order to remove feldspars and etch quartz grains, the remaining part of the sample was then treated with 40% HF for 40 min. The samples were then placed again into 40% HCl for >4 h to subtract fluorides produced by the former HF treatment. Subsequently, the samples were washed with distilled water to neutralise the



Fig 1. Geological setting and sampled terrace profiles of the upper Han River, China.

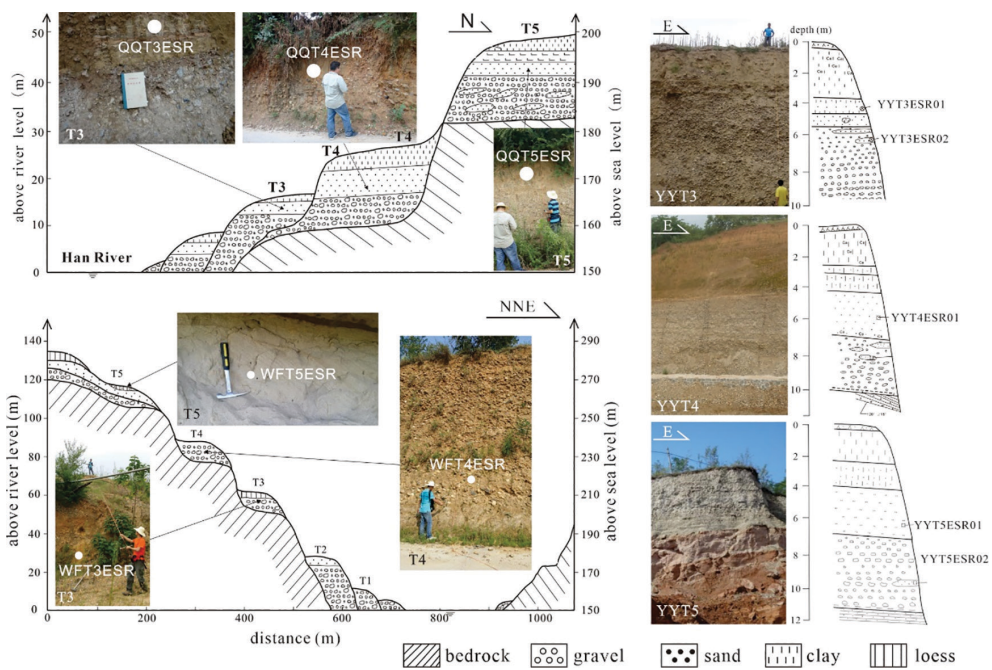


Fig 2. Sketch map showing the sampling profile stratigraphy and field photographs of the Wufeng, Qingqu and Yuyang terrace systems of the upper Han River, China.

Table 1. Results of ESR dating for the Wufeng, Qingqu, and Yunyang Basin terraces in the upper Han River valley.

Sampling profile	Terrace level	Sample no.	Above sea level (m)	Thick of the profile	U (ppm)	Th (ppm)	K (%)	Water content (%)	Dose rate (Gy/ka)	De (Gy)	Age (ka)
Wufeng terrace profile	T3	WFT3ESR	215	9	3.00 ± 0.11	15.20 ± 0.05	2.07 ± 0.08	18 ± 3	3.04 ± 0.15	1269 ± 145	417 ± 48
	T4	WFT4ESR	235	10	2.57 ± 0.11	14.10 ± 0.05	2.91 ± 0.05	17 ± 3	3.58 ± 0.18	2246 ± 348	627 ± 97
	T5	WFT5ESR	277	15	2.35 ± 0.11	12.41 ± 0.05	2.47 ± 0.05	18 ± 3	3.05 ± 0.15	3371 ± 556	1105 ± 182
Qingqu terrace profile	T3	QUT3ESR	175	14	2.90 ± 0.11	14.80 ± 0.05	1.97 ± 0.05	16 ± 3	3.00 ± 0.15	1214 ± 123	405 ± 41
	T4	QUT4ESR	203	5	2.65 ± 0.11	13.30 ± 0.05	2.15 ± 0.05	17 ± 3	2.96 ± 0.15	1840 ± 227	622 ± 77
Yunyang basin terrace profile	T5	QUT5ESR	249	23	2.06 ± 0.11	13.29 ± 0.05	2.25 ± 0.05	16 ± 3	2.96 ± 0.15	3343 ± 359	1129 ± 121
	T3	YTT3ESR	165	20	3.00 ± 0.11	15.40 ± 0.05	1.98 ± 0.05	18 ± 3	2.98 ± 0.15	1258 ± 199	422 ± 67
	T3	YTT3ESR	167	20	2.90 ± 0.11	16.00 ± 0.05	1.96 ± 0.05	18 ± 3	2.98 ± 0.15	1194 ± 175	401 ± 59
	T4	YTT4ESR	232	24	2.57 ± 0.11	13.70 ± 0.05	2.22 ± 0.05	16 ± 3	3.07 ± 0.15	1905 ± 161	621 ± 52
	T5	YTT5ESR	274	6	2.34 ± 0.11	11.8 ± 0.05	2.39 ± 0.05	18 ± 3	2.96 ± 0.15	3261 ± 475	1102 ± 160
	T5	YTT5ESR	275	6	2.41 ± 0.11	11.81 ± 0.05	2.47 ± 0.05	17 ± 3	3.07 ± 0.15	3375 ± 360	1099 ± 117

ESR, electron spin resonance.

acid and dried at low temperature (~43°C) for over 24 h. X-ray diffraction analytical results revealed that the purified quartz from 11 samples had high purity ranging from 97.19% to 99.99%.

3.2. Gamma-Ray Radiation Dose

Quartz grains were dated by the ESR method using the multiple-aliquot additive dose method of Ti-related centres (Toyoda *et al.*, 2000; Duval and Guilarte, 2015). Irradiation was performed using the ⁶⁰Co source of the laboratory of Peking University, Beijing, China, with a dose rate of 42.25 Gy/min. Each sample was divided into 10 aliquots for irradiation at the expected doses of 0 Gy, 237.65 Gy, 433.1 Gy, 863.7 Gy, 1677.5 Gy, 2662.5 Gy, 3798 Gy, 4887 Gy, 6512.5 Gy and 8811.5 Gy, calibrated using reference standard alanine dose tablets.

3.3. ESR Measurements

The ESR measurements were conducted using a BRUKER EPR041XG X-band spectrometer cooled to 77 K with liquid nitrogen in a finger-dewar at the State Key Laboratory of Earthquake Dynamics, Institute of Geology, China Earthquake Administration, Beijing, China. ESR measurements of the Ti–Li centre were performed with a microwave power of 5 mW and modulation amplitude of 0.16 mT. For the Ti–Li centre, ESR signal intensity was measured from the top of the peak at g = 1.979 to the bottom at g = 1.913 (Fig. 3; Rink *et al.*, 2007; Tissoux *et al.*, 2007; Liu *et al.*, 2010; Duval and Guilarte, 2015). Given the anisotropy of the ESR signal intensity, each aliquot was measured at six angles (~60° interval) in the cavity, with the mean value being calculated to reduce the variation caused by the anisotropy of quartz.

3.4. Equivalent-Dose Determination

In the present work, SSE functions were applied to the Ti–Li centre data to determine the equivalent dose (Woda and Wanger, 2007; Duval and Guilarte, 2015; Wei *et al.*, 2020). The goodness of fit of these functions was assessed using the error coefficient and adjusted R-square. Equations of the fitting functions and all DRCs of all samples are shown in Fig. 4.

3.5. Dose Rate Calculation

Contents of uranium (U) and thorium (Th) were measured using inductively coupled plasma–mass spectrometry, and potassium (K) was measured using inductively coupled plasma–optical emission spectrometry at Chang’an University, Xi’an, China. Water content was measured by weighing the samples, which were taken from the same location as the dated samples, before and after drying. The cosmic ray dose rate was estimated for each sample as a function of depth, altitude and geomagnetic latitude

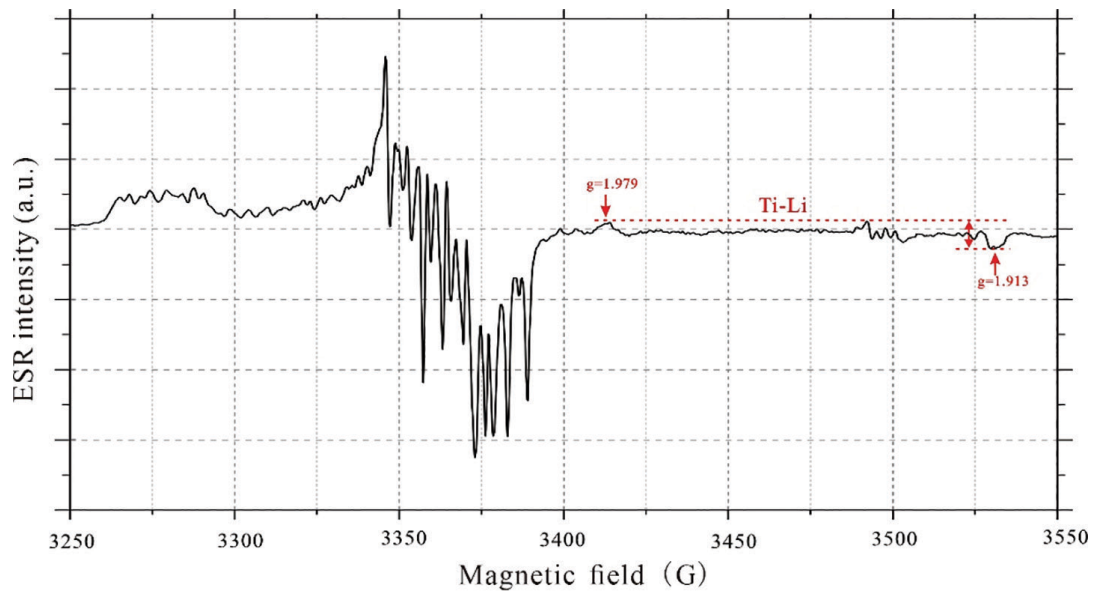


Fig 3. ESR spectrum showing the method used to determine the ESR signal intensity of the Ti-Li centre. Red arrows represent the measurement positions and g values of the Al and Ti-Li centres. ESR, electron spin resonance.

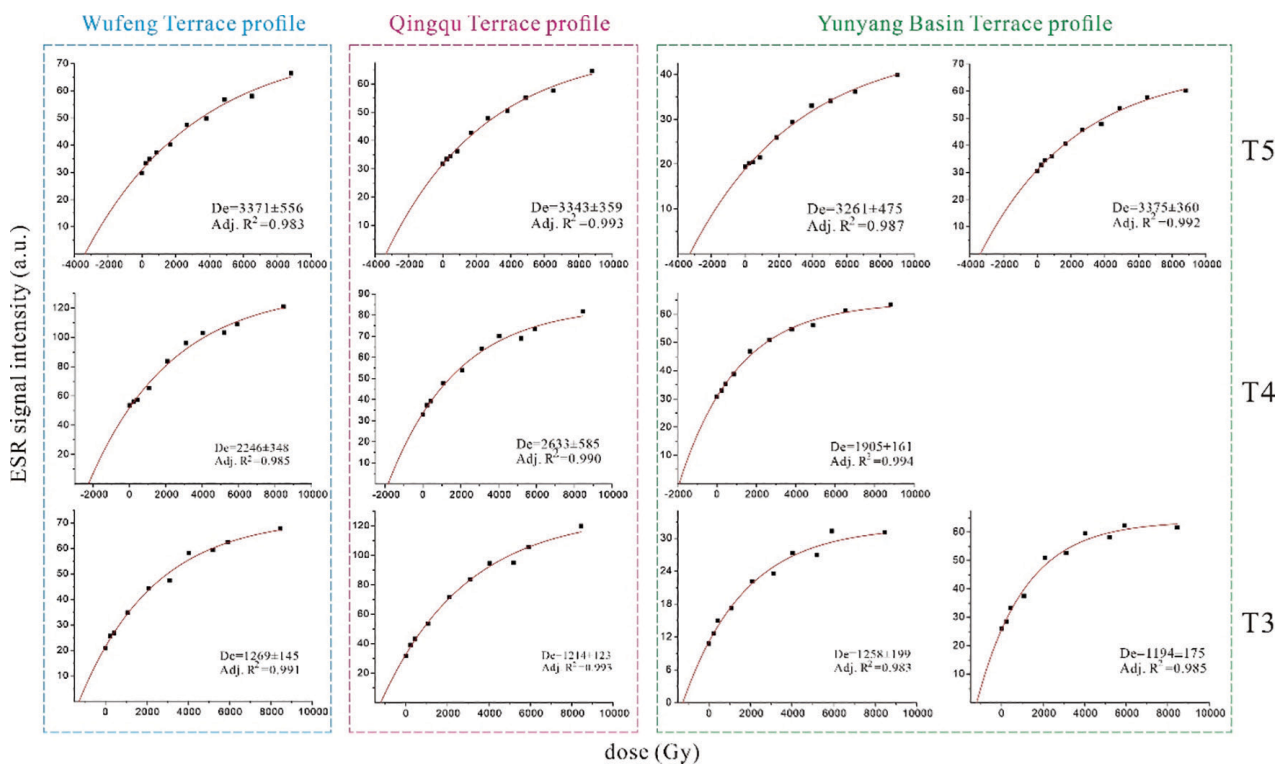


Fig 4. Dose–response curves of the quartz Ti-Li centre for samples collected from terraces T3–T5 of the upper Han River. ESR, electron spin resonance.

according to Prescott and Hutton (1994). Total dose rates were calculated using the conversion factors of Guérin *et al.* (2011), and the results are provided in **Table 1**.

4. Results and Discussions

4.1. Distribution of Terraces

Field investigation and digital elevation model terrain analyses show that five terrace levels are widely distributed in the Han River study area (**Fig. 1**). The elevations of the sampled terraces in each of the three studied profiles are given in **Table 1**. The higher terraces T3–T5 can be recognised as flat landforms distributed continuously over long distances. Each terrace is composed of coarse-gravel layers and fine-sand lenses, which are partly covered by loess layers (**Fig. 2**). Those fluvial–lacustrine deposition characteristics are similar to the terrace sedimentary of the upper Jinsha River (Wei *et al.*, 2023). The fine loess is not suitable for extracting quartz for ESR dating; therefore, sand from lenses in the fluvial–lacustrine sediments was collected for ESR dating.

4.2. ESR Dating Results

Wei *et al.* (2020) showed that the Ti–Li centre ESR signal intensity of present-day Yangtze River fluvial sediments was zeroed by sunlight before burial. The sediment of the Han River, which is a major tributary of the Yangtze River, undergoes sediment transportation mainly by saltation (Sun *et al.*, 2020), which favours zeroing of the ESR signal. Therefore, we consider that the quartz ESR signal of the Han River terrace samples was zeroed. In addition, **Fig. 4** shows that the quartz ESR signal intensity increases markedly with increasing γ -ray dose. All of these data indicate that our ESR ages are reliable (**Table 1**). The ESR ages and uncertainties for T3, T4 and T5 of the Wufeng terrace profile are 417 ± 48 ka, 627 ± 97 ka and 1105 ± 182 ka, respectively; those for T3, T4 and T5 of the Qingqu terrace profile are 405 ± 41 ka, 622 ± 77 ka and 1129 ± 121 ka, respectively;

and those for T3, T4 and T5 of the Yunyang Basin terrace profile are 422 ± 67 ka to 401 ± 59 ka, 621 ± 52 ka and 1102 ± 60 ka to 1099 ± 117 ka, respectively.

4.3. Formation Ages of Terraces T3–T5 of the Upper Han River

We compared our ESR ages with previously determined OSL dating results for T1–T2 and paleo-magnetic dating results for the higher-level terraces. Pang *et al.* (2015) determined an age of 55–25 ka for T1, and Zhu *et al.* (2022) estimated an age of 220–180 ka for T2. Van Buren *et al.* (2020) determined an age of 693–625 ka for T3. Results of stratigraphic correlation have given age estimates for T4, T5 and T6 of 1.05–0.78 Ma, ~1.5 Ma and 1.82 Ma, respectively (Sun *et al.*, 2017a,b; Zhu *et al.*, 2023).

The results of our field investigation (see **Fig. 2**) show that the fluvial–lacustrine sediments at the same altitude of various terraces directly overlie bedrock; therefore, the samples collected are of ancient terrace deposits. In summary, our dating results show that the ESR central ages of terrace quartz sediments for each of T3, T4 and T5 in the three studied terrace profiles are highly consistent, in the ranges of 422–401 ka for T3, 627–621 ka for T4 and 1129–1099 ka for T5.

4.4. Mechanism of Formation of Higher Terraces of the Upper Han River

The evolution of fluvial systems is highly sensitive to climate change, including the formation and preservation of terraces (Vandenberghe, 2003; Winsemann *et al.*, 2015). In **Fig. 5**, we compare the formation ages of the upper Han River terraces with the deep-ocean oxygen isotope curve, which is a proxy for paleo-climatic conditions. This figure shows that it is only T3 and T4, but it is likely for all the dated terraces of the upper Han River to have formed during the transition from a glacial to interglacial period. This correspondence is consistent with rivers originating from mountain systems in temperate regions (Hatten *et al.*, 2012). Indeed, changes in monsoon climate and vegetation

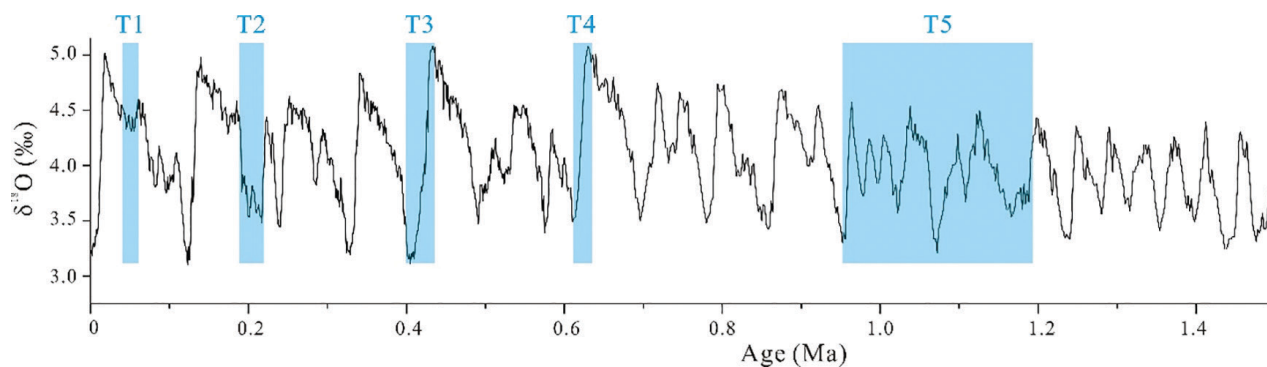


Fig 5. Correspondence between the ages of upper Han River terraces and climate change recorded by marine $\delta^{18}\text{O}$.

have also resulted in changes in river runoff and sediment volume in the past (Zhang *et al.*, 2023). During glacial–interglacial transitions, the moderate sediment supply would have led to partial exposure of the riverbed and strengthened undercutting, allowing terrace systems to form (Wang *et al.*, 2015, 2021).

The age range (central value range) for the formation of terrace T5 determined in this study is 1129–1099 ka (i.e., slightly younger than ~1.2 Ma), which corresponds to the early stage of the mid-Pleistocene transition (MPT), when the periodicity of Pleistocene glacial cycles changed from ~41 ka to ~100 ka. It is possible that the small amplitude and short duration of climatic cycles before this time disfavoured the formation and preservation of terraces prior to the formation of T5. This interpretation is supported by studies of terrace sediments in other locations, which have indicated the terrace formation since the MPT has been closely related to the 100 ka climatic cycle (Bridgland *et al.*, 2008). In addition, the increase in amplitude and duration of climatic cycles since the MPT may have led to phases of more intense river erosion and accumulation. This might explain why terraces were formed and preserved after 1.2 Ma (but not before) in the upper section of the Han River.

Uplift of the eastern Qin Mountains since 1.2 Ma has also influenced the development of the Han River terraces (Liu, 2004; Sun *et al.*, 2016). High rates of tectonic uplift are inferred to have led to substantial elevation differences between river terrace levels and amplified the influence of climate change on the sedimentation–erosion process of the river, leading to the development and preservation

of flights of terraces (Wang *et al.*, 2015). In summary, after 1.2 Ma, the rates of uplift and erosion increased, and terrace systems were formed in the upper Han River, with cyclic climatic transitions amplifying these effects on terrace formation.

5. Conclusions

In this study, through detailed field investigation, ESR dating and stratigraphic correlation, we determined the formation ages of the Quaternary higher terraces (T3–T5) of the upper Han River, central China. Terraces T3, T4 and T5 were formed at 422–401 ka, 627–621 ka and 1129–1099 ka, respectively. The formation times of the terraces correspond to glacial–interglacial transitions identified in the marine oxygen isotope record. Terrace T5 (i.e., the highest terrace) formed just after 1.2 Ma, which was the start time of the MPT. Integrating this information with the recorded uplift of the eastern Qin Mountains since 1.2 Ma, we propose that the terrace sequence of the upper Han River formed as a result of the combined effect of climatic transition and tectonic uplift.

Acknowledgements

This work was supported by the National Non-profit Fundamental Research Grant of China, China Earthquake Administration (No. 1521401800062).

References

- Bahain JJ, Shao QF, Han F, Sun XF, Voinchet P, Liu CR, Yin GM and Falgueres C, 2017. Contribution des méthodes ESR et ESR/U-Th à la datation de quelques gisements pléistocènes de Chine. *L'anthropologie* 121(3): 215–233, DOI 10.1016/j.anthro.2017.06.001.
- Beerten K, Lomax J, Clémer K, Stesmans A and Radtke U, 2006. On the use of Ti centres for estimating burial ages of Pleistocene sedimentary quartz: Multiple-grain data from Australia. *Quaternary Geochronology* 1(2): 151–158, DOI 10.1016/j.quageo.2006.05.037.
- Bridgland D, Westaway R, 2008. Climatically controlled river terrace staircases: a worldwide Quaternary phenomenon. *Geomorphology* 98(3–4): 285–315.
- Chen TM, Yang Q, Hu YQ, Bao WB and Li TY, 1997. ESR dating of tooth enamel from yunxian homo erectus site, China. *Quaternary Science Reviews* 16(3–5): 455–458.
- Duval M and Guilarte V, 2015. ESR dosimetry of optically bleached quartz grains extracted from Plio-Quaternary sediment: Evaluating some key aspects of the ESR signals associated to the Ti-centres. *Radiation Measurements* 78: 28–41, DOI 10.1016/j.radmeas.2014.10.002.
- Guérin G, Mercier N and Adamiec G, 2011. Dose-rate conversion factors: Update. *Ancient TL* 29(1): 5–8.
- Hatten JA, Goñi MA and Wheatcroft RA, 2012. Chemical characteristics of particulate organic matter from a small, mountainous river system in the Oregon Coast Range, USA. *Biogeochemistry* 107: 43–66.
- Huang PH and Li WS, 1995. Landscape, Quaternary strata and buried environment at estuary of the Quyuan River in Yunxian County, Hubei Province. *Jiangnan Archaeology* (4): 83–86, DOI CNKI: SUN: JHKG.0.1995-04-012.
- Huang XS, Zheng SH, Li CR, Zhang ZQ, Guo JW and Liu LP, 1996. Discovery of vertebrate fossils and paleolithic artifacts in Danjiang submerging area and its implications. *Vertebrata Palasiatica* 34(3): 228–233, DOI 10.19615/j.cnki.1000-3118.1996.03.009.

- Liu CR, Yin GM, Gao L, Bahain JJ, Li JP and Lin M, 2010. ESR dating of Pleistocene archaeological localities of the Nihewan basin, north china-preliminary results. *Quaternary Geochronology* 5(2–3): 385–390, DOI 10.1016/j.quageo.2009.05.006.
- Liu HJ, 2004. Formation and Evolution of Weihe River Basin and Uplift of Eastern Qinling Mountains. Northwest University, Xi'an.
- Luo XK, Yin ZQ and Yang LW, 2019. Preliminary analysis on the development characteristics of river terraces and their relationship with ancient landslides in the upper section of Minjiang River. *Quaternary Sciences* 39(2): 391–398, DOI 10.11928/j.issn.1001-7410.2019.02.11.
- Mao PN, Pang JL, Huang CC, Zha XC, Zhou YL and Guo YQ, 2017. Loess deposits of the upper Hanjiang River valley, south of Qinling Mountains, China: Implication for the pedogenic dynamics controlled by paleomonsoon climate evolution. *Aeolian Research* 25: 63–77, DOI 10.1016/j.aeolia.2017.03.001.
- Meng QR, 2017. Origin of the Qinling Mountains. *Science China: Earth Sciences* 47(4): 412–420, DOI CNKI:SUN:JDXK.0.2017-04-005.
- Mao PN, Pang JL, Huang CC, Zhou YL, Zha XC, Zhang WT and Guo YQ, 2017. Climate change during the late stages of MIS3 period inferred from the loess record in the upper Hanjiang River valley. *Quaternary Sciences* 37(3): 535–547, DOI 10.11928/j.issn.1001-7410.2017.03.10.
- Pang JL, Huang CC, Zha XC, Zhou YL, Qiao J and Zhao YL, 2013. Soil diagnostic horizon characteristics and its significance in the upper Hanjiang valley, China. *Acta Pedologica Sinica* 50(6): 1082–1089, DOI 10.11766/trxb201301130026.
- Pang JL, Huang CC, Zhou YL, Zha XC, Qiao J, Zhang YZ and Zhou L, 2014. Formation of the first river terraces of Hanjiang River and its response to the East Asian monsoon changes. *Geological Review* 60(5): 1076–1084, DOI 10.3969/j.issn.0371-5736.2014.05.011.
- Pang JL, Huang CC, Zhou YL, Zha XC, Zhang WT, Cui TY and Mao PN, 2017. OSL dating of the Tuojiawan loess-palaeosol profile and climatic change during the last 55 ka BP. *Acta Geologica Sinica* 91(12): 2841–2853, DOI 10.3969/j.issn.0001-5717.2017.12.018.
- Pang JL, Huang CC, Zhou YL, Zha XC, Zhang YZ and Wang LB, 2015. Eolian loess palaeosol sequence and OSL age of the first terraces within the Yunxian Basin along the upper Hanjiang River. *Acta Geographica Sinica* 70(1): 63–72, DOI 10.11821/dlxb201501005.
- Prescott JR and Hutton JT, 1994. Cosmic ray contributions to dose rates for luminescence and ESR dating: Large depths and long-term time variations. *Radiation measurements* 23(2–3): 497–500. DOI 10.1016/1350-4487(94)90086-8.
- Rink WJ, Bartoll J, Schwarcz HP, Shane P and Bar-Yosef O, 2007. Testing the reliability of ESR dating of optically exposed buried quartz sediments. *Radiation Measurements* 42(10): 1618–1626, DOI 10.1016/j.radmeas.2007.09.005.
- Starkel L, 2003. Climatically controlled terraces in uplifting mountain areas. *Quaternary Science Reviews* 22(20): 2189–2198, DOI 10.1016/S0277-3791(03)00148-3.
- Sun XF, Jia X, Lu HY, Wang XY, Yi SW, Wang XY, Xu ZW, Lei F and Han ZY, 2017a. A modified depositional hypothesis of the Hanjiang Loess in the southern Qinling Mountains, central China. *Progress in Physical Geography: Earth and Environment* 41(6): 775–787, DOI 10.1177/0309133317738711.
- Sun XL, Kuiper KF, Tian YT, Li CA, Gemignani L, Zhang ZJ and Wijbrans JR, 2020. Impact of hydraulic sorting and weathering on mica provenance studies: An example from the Yangtze River. *Chemical Geology* 532: 119359, DOI 10.1016/j.chemgeo.2019.119359.
- Sun XF, Li YH, Feng XB, Lu CQ, Lu HY, Yi SW, Wang SJ and Wu SY, 2016. Pedostratigraphy of aeolian deposition near the Yunxian Man site on the Hanjiang River terraces, Yunxian Basin, central China. *Quaternary International* 400: 187–194.
- Sun XF, Lu HY, Wang SJ and Yi SW, 2012. Ages of Liangshan Paleolithic sites in Hanzhong Basin, Central China. *Quaternary Geochronology* 10: 380–386, DOI 10.1016/j.quageo.2012.04.014.
- Sun XF, Lu HY, Wang SJ, Yi L, Li YX, Bahain JJ, Voinchet P, Hu XZ, Zeng L and Zhang WC, 2017b. Early human settlements in the southern Qinling Mountains, central China. *Quaternary Science Reviews* 164: 168–186, DOI 10.1016/j.quascirev.2017.04.005.
- Tao YL, Chang H and Qiang XK, 2018. Terraces and their chronology features of the First Bend along the Changjiang River. *Quaternary Sciences* 38(1): 151–164, DOI 10.11928/j.issn.1001-7410.2018.01.13.
- Tissoux H, Alguères CF, Voinchet P, Toyoda S, Bahain JJ and Desprée J, 2007. Potential use of Ti-center in ESR dating of fluvial sediment. *Quaternary Geochronology* 2(1–4): 367–372, DOI 10.1016/j.quageo.2006.04.006.
- Tissoux H, Toyoda S, Falguères C, Voinchet P, Takada M, Bahain JJ and Desprée J, 2008. ESR dating of sedimentary quartz from two Pleistocene deposits using Al and Ti-centers. *Geochronometria* 30: 23–31, DOI 10.2478/v10003-008-0004-y.
- Tissoux H, Valladas H, Voinchet P, Reyss JL, Mercier N, Falguères C, Bahain JJ, Zoller L and Antoine P, 2010. OSL and ESR studies of aeolian quartz from the Upper Pleistocene loess sequence of Nussloch (Germany). *Quaternary Geochronology* 5(2/3): 131–136, DOI 10.1016/j.quageo.2009.03.009.
- Toyoda S, Voinchet P, Falguères C, Dolo JM and Laurent M, 2000. Bleaching of ESR signals by the sunlight: A laboratory experiment for establishing the ESR dating of sediments. *Applied Radiation and Isotopes* 52(5): 1357–1362.
- Van Buuren U, Prins MA and Wang XY, Stange M, Yang X, van Balen RT, 2020. Fluvial or aeolian? Unravelling the origin of the silty clayey sediment cover of terraces in the Hanzhong Basin (Qinling Mountains, central China). *Geomorphology* 367: 107294, DOI 10.1016/j.geomorph.2020.107294.

- Vandenberghe J, 2003. Climate forcing of fluvial system development: An evolution of ideas. *Quaternary Science Reviews* 22(20): 2053–2060, DOI 10.1016/S0277-3791(03)00213-0.
- Voinchet P, Despriée J, Tissoux H, Falguères C, Bahain JJ, Gageonnet R, Depont J and Dolo JM, 2010. ESR chronology of alluvial deposits and first human settlements of the Middle Loire Basin (Region Centre, France). *Quaternary Geochronology* 5(2/3): 381–384, DOI 10.1016/j.quageo.2009.03.005.
- Voinchet P, Falguères C, Tissoux H, Bahain JJ, Despriée J and Pirouelle F, 2007. ESR dating of fluvial quartz: Estimate of the minimal distance transport required for getting a maximum optical bleaching. *Quaternary Geochronology* 2(1/2/3/4): 363–366, DOI 10.1016/j.quageo.2006.04.010.
- Voinchet P, Toyoda S, Falguères C, Marion H, Hélène T, Davinia M and Jean-Jacques B, 2015. Evaluation of ESR residual dose in quartz modern samples, an investigation on environmental dependence. *Quaternary Geochronology* 30: 506–512, DOI 10.1016/j.quageo.2015.02.017.
- Wang BL, Wang XY, Yi SW, Zhao L and Lu HY, 2021. Responses of fluvial terrace formation to monsoon climate changes in the north-eastern Tibetan Plateau: Evidence from pollen and sedimentary records. *Palaeogeography, Palaeoclimatology, Palaeoecology* 564: 110196, DOI 10.1016/j.palaeo.2020.110196.
- Wang XY, Vandenberghe J, Yi SW, Van Balen R and Lu HY, 2015. Climate-dependent fluvial architecture and processes on a suborbital timescale in areas of rapid tectonic uplift: An example from the NE Tibetan Plateau. *Global and Planetary Change* 133: 318–329, DOI 10.1016/j.gloplacha.2015.09.009.
- Wang YG, Chang H and Zhou WJ, 2021. Fluvial terrace evolution and its tectonic-climatic significance in the Weihe Basin. *Geological Review* 67(4): 1033–1049, DOI 10.16509/j.georeview.2021.04.305.
- Wei CY, Voinchet P, Zhang YF, Bahain JJ, Liu CR, Kang CG, Yin GM, Sun XL and Li CA, 2020. Chronology and provenance of the Yichang Gravel Layer deposits in the Jiangnan Basin, middle Yangtze River Valley, China: Implications for the timing of channelization of the Three Gorges Valley. *Quaternary International* 550: 39–54, DOI 10.1016/j.quaint.2020.03.020.
- Wei CY, Yin GM, Du JH, Liu CR, Cheng L, Ji H and Wang LB, 2023. Residual electron spin resonance signals of quartz from the 2018 Baige dammed lake in Tibet: Implications for the identification of sediment layers caused by megafloods. *Frontiers in Earth Science* 10: 1035655, DOI 10.3389/feart.2022.1035655.
- Winsemann J, Lang J, Roskosch J, Polom U, Böhner U, Brandes C, Glotzbach C and Frechen M, 2015. Terrace styles and timing of terrace formation in the Weser and Leine valleys, northern Germany: Response of a fluvial system to climate change and glaciation. *Quaternary Science Reviews* 2015(123): 31–57, DOI 10.1016/j.quascirev.2015.06.005.
- Woda C and Wagner GA, 2007. Non-monotonic dose dependence of the Ge- and Ti-centres in quartz. *Radiation measurements* 42(9): 1441–1452, DOI 10.1016/j.radmeas.2007.03.003.
- Xue XX, Li HH, Li YX and Liu HJ, 2004. The new data of the uplifting of Qinling Mountains since the middle Pleistocene. *Quaternary Sciences* 24(1): 82–87, DOI 10.3321/j.issn:1001-7410.2004.01.010.
- Zeuner FE, 1935. The Pleistocene chronology of Central Europe. *Geological Magazine* 72(8): 350–376.
- Zhang GW, Guo AL, Dong YP and Yao AP, 2019. Rethinking of the Qinling orogen. *Journal of Geomechanics* 25(5): 746–768, DOI 10.12090/j.issn.1006-6616.2019.25.05.064.
- Zhu YY, Zhou YL, Yang JM, Jia BB, Pang JL, Cui YY, Yan XJ, Sun XW and Zhang YM, 2022. Optical luminescence dating research of the second terrace in the upper Hanjiang River. *Quaternary Sciences* 42(5): 1260–1276, DOI 10.11928/j.issn.1001-7410.2022.05.03.
- Zhu ZD, 1955. Valley landscape of Hanjiang river upstream between Danjiangkou to Baihe. *Acta Geographica Sinica* 21(03): 259–271, DOI 10.11821/xb195503003.